

Einstein-Cartan cosmology and the high-redshift Universe

DAVOR PALLE

ul. Ljudevita Gaja 35, 10000 Zagreb, Croatia [†]

The Hubble tension, known as a discrepancy between the local measurements vs. the CMB, SNe and galaxy clustering fits of the Hubble constant, the first measurement of the 21-centimeter high-redshift signal by EDGES and the high-redshift galaxy halo number densities, represent a great challenge for the concordance cosmology. We show that light and heavy Majorana neutrinos embedded into the Einstein-Cartan cosmology resolve the main obstacles of the concordance cosmological model.

PACS numbers: 04.50.Kd Modified theories of gravity; 12.15.-y Electroweak interactions; 98.62.Gq Galactic halos; 98.80.-k Cosmology

1. Introduction and motivation

The General Relativity (GR), the cosmological constant and the cold dark matter (CDM) are the fundamental building blocks of the Λ CDM concordance cosmological model adopted to reproduce satisfactorily a large number of cosmological phenomena [1, 2, 3, 4]. However, abundant new measurements of high-redshift quasars and galaxies, 21-centimeter absorption signal, precise local Hubble constant measurements against those inferred from the CMB, lensing, SNe or galaxy clustering and a notorious lack of the large scale power of CMB spectrum, dictate to inevitable need to substantially improve or even completely replace the Λ CDM model.

In this paper we explicate and illuminate the possibility how to comprehend the appearance of dark matter and dark energy starting from the nonsingular and causal theories in the local Minkowski frame and in the global curved space-time. The next chapter is devoted to a description of the particle content of the Universe, demonstrating also the difference from the Standard Model (SM) of particle physics.

[†] email: davor.palle@gmail.com

2. Particle content of the Universe

Intending to remove the ultraviolet-UV (zero-distance) singularity and the SU(2) global anomaly, a new theory of the local relativistic quantum fields is formulated in [5]. We show in [5] the intricate relations between gauge, discrete and conformal symmetries in Minkowski space-time and how to acquire electromagnetic, weak and strong interactions embedded into the conformal SU(3) gauge symmetry.

The spectrum of the theory can be revealed within the study of Dyson-Schwinger equations with the UV cut-off defined by the mass of weak gauge W and Z bosons $\Lambda = \frac{\pi}{\sqrt{6}} \frac{2}{g} M_W$, $e = g \sin \Theta_W$, $\cos \Theta_W = \frac{M_W}{M_Z}$. Instead of the SM massless Dirac neutrinos, the theory of ref. [5] contains light and heavy Majorana neutrinos. The weak boson mixing angle and quark (lepton) mixing angles must fulfill the following relation in order to preserve a cancelation of the fermion and boson SU(2) global anomalies [5]:

$$\Theta_W = 2(\Theta_{12}^D + \Theta_{23}^D + \Theta_{31}^D). \quad (1)$$

This relation must be valid even for Majorana neutrinos. Namely, in the case of the inverted mass hierarchy, for example if $m_{\nu,1}^M > m_{\nu,2}^M$ for light Majorana neutrinos, $m_{N,1}^M < m_{N,2}^M$ for heavy Majorana neutrinos and $m_{\nu,1}^D < m_{\nu,2}^D$ for Dirac neutrinos, the see-saw mechanism and the Euler matrix imply $\Theta_{12}^D = -\Theta_{12}^M$:

$$\begin{pmatrix} \cos \Theta_{12} & \sin \Theta_{12} \\ -\sin \Theta_{12} & \cos \Theta_{12} \end{pmatrix} \begin{pmatrix} u_1 \\ u_2 \end{pmatrix} \Leftrightarrow \begin{pmatrix} \cos \Theta_{12} & -\sin \Theta_{12} \\ \sin \Theta_{12} & \cos \Theta_{12} \end{pmatrix} \begin{pmatrix} u_2 \\ u_1 \end{pmatrix}.$$

Before checking the relation between boson and fermion mixing angles, one has to verify the unitarity of the quark and lepton mixing matrices.

Very strong coupling of heavy Majorana neutrinos and Nambu-Goldstone scalars ensures very large masses [5]. Light and heavy Majorana neutrinos are cosmologically stable particles, i.e. $\tau_{N_i}, \tau_{\nu_j} > \tau_U$ [6]. Furthermore, heavy Majorana neutrinos are perfect candidates for the CDM particles [7] that simultaneously solve the leptogenesis [8] and baryogenesis problems since $\Delta L = \Delta B$ [2] in the (denoted as BY) theory of ref. [5]. CP violation in lepton and baryon processes is mandatory [9].

The particle content of the BY theory has all cosmological ingredients such as CDM, small amount of hot dark matter (light neutrinos) and lepton (baryon) number violation, therefore just everything what the SM does not contain.

The UV cut-off $\Lambda = 326 GeV = 0.6 \times 10^{-16} cm$ as a dimensionful parameter of the noncontractible space breaks the gauge, conformal and discrete

symmetries, and it causes profound phenomenological consequences in particle physics. Flavour anomalies in suppressed B meson decays [10, 11] or few QCD anomalies [12, 13] are a matter of intense experimental investigations.

The proclaimed discovery of the 125 GeV Higgs scalar of the SM cannot be considered as a final assertion. Namely, 125 GeV resonance can be interpreted as a scalar meson by coupling scalar toponium and gluonium bound states [14, 15]. The additional 750 GeV scalar resonance can be found only with very large datasets because only gluonium part can be detected above toponium threshold. Namely, it is very well known that t-quark decays faster than the occurrence of the hadronization process. Similar type of hadron resonances can be expected from the mixture of bottomonium and gluonium. It is advantageous that numerical simulations with lattice QCD and b-quarks are feasible. Assuming the strong coupling of heavy quarkonia and gluonium (i.e. large annihilation matrix element [15]) and $A(t\bar{t}, gg)/m(t\bar{t}) \simeq A(b\bar{b}, gg)/m(b\bar{b})$, the scalar bottomonium-gluonium $\simeq 30$ GeV heavy resonance could appear [16].

3. Introducing the Einstein-Cartan cosmology

Initial conditions of the singular Λ CDM cosmology are established with the introduction of the inflaton scalar [2, 4]. The parameters of inflation are fine tuned to solve various problems of the expanding GR cosmology. The total density normalized to the critical density is predicted to be $\Omega_{tot} = 1$, but the mass density and cosmological constant are obtained as a fit to data, not as a firm prediction of the inflation and Λ CDM cosmology.

The Einstein-Cartan theory of gravity (cosmology) presents the generalization of the GR by including rotational degrees of freedom [17]. The first important cosmological result for Einstein-Cartan(EC) cosmology was proved by A. Trautman [18] demonstrating how to avoid a singularity by a torsion.

To envisage the evolution of the Universe from some R_{min} to $R = \infty$, we recall the reader to, for example, integral Dyson-Schwinger equation in Minkowski space-time for some fermion. Any solution of this integral equation in the space-like domain ($0 \leq -q^2 \leq \Lambda^2$) at some particular space-time point is defined by a behaviour in the whole space-like domain. This is a bootstrap character of Dyson-Schwinger integral equation. A continuation to the time-like domain to gain the spectrum of the fermion requires solutions in both space-like and time-like domains. We suspect that some kind of bootstrap exist within EC cosmology.

Verifying that the EC cosmology has $R_{min} \simeq \mathcal{O}(10^{-16}cm)$ [19], we show that quantum fluctuations at R_{min} generate primordial density fluctuations [20, 21]. During the era of the CDM matter (heavy Majorana neutrinos)

decoupling, the abundant number of right-handed helicity(chirality) light neutrinos are created [22]. Important to restate that heavy Majorana neutrinos are responsible for lepton and baryon number violations [8]. All particles must fulfill EC equations of motion:

$$\begin{aligned} \frac{d^2 x^k}{ds^2} + \Gamma_{(ij)}^k \frac{dx^i}{ds} \frac{dx^j}{ds} &= 0, \quad (ij) = \frac{1}{2}(ij + ji), \quad (2) \\ \Gamma_{(ij)}^k &= \left\{ \begin{matrix} k \\ ij \end{matrix} \right\} + 2S_{(ij)}^k, \quad \Gamma_{ij}^k = \left\{ \begin{matrix} k \\ ij \end{matrix} \right\} + S_{ij}^k - S_{ji}^k + S_{ij}^k, \\ \text{torsion tensor} &= S_{ij}^k = \frac{1}{2}(\Gamma_{ij}^k - \Gamma_{ji}^k) = \Gamma_{[ij]}^k. \end{aligned}$$

Because of the right-handed chirality light neutrino number and spin density dominance at early times of evolution and EC equations of motion with torsion term, violation of isotropy inevitably occurs. Averaged spin (torsion) of matter (space-time) cannot be erased in the ongoing evolution. Small at early times, after creation of larger and larger structures (stars, globular clusters, galaxies, clusters, superclusters), torsion is now proportional to the angular momentum of the Universe with right handed chirality [22].

Let us denote the cosmic scale factor by $a(z) = 1/(1+z) = R(t)/R_0$. The evolution from the present state to infinity is then for $a \in [1, \infty)$, $z \in (-1, 0]$. Acknowledging the state of the Universe in the cosmology in the vicinity of spacelike infinity [23] and conformal technique of Penrose [24] we come to the following conclusions [19, 21]:

$$\begin{aligned} \lim_{R \rightarrow \infty} \frac{\rho_m}{\rho_{crit}} &= 2, \quad \lim_{R \rightarrow \infty} \frac{\rho_Q}{\rho_{crit}} = -1, \quad \lim_{R \rightarrow \infty} \frac{\rho_\Lambda}{\rho_{crit}} = 0, \\ \Omega_{cmb} = \mathcal{O}(10^{-4}) &\ll 1 \Rightarrow \Omega_m = 2, \quad \Omega_Q = -1, \quad \Omega_\Lambda = 0. \end{aligned}$$

Precisely at this point one can observe the action of bootstrap: matter density contributes to the curvature but the negative opposing contribution of the angular momentum of matter through torsion-bootstrap action infers to equality of the total and critical densities.

Summarizing all results of the EC cosmology we conclude that there is no need for the inclusion of the inflaton scalar (after all R_{min} is at the weak interaction scale not at the Planck scale) since we can generate primordial perturbations and anisotropy through torsion. Moreover, we fix even matter density.

We need to model the evolution of torsion (angular momentum) of the Universe in order to perform numerical evaluations in the next chapter. The

Table 1. Model parameters.

model	Ω_m	Ω_Λ	h	c	$z_0; z_1$	τ_U	Ω_b
Λ CDM	0.307	0.693	0.677	-	-	13.83 Gyr	0.045
EC	2	0	0.74	1.85	4;6	13.92 Gyr	0.045

most natural method is to equate the ages of the Universe for Λ CDM and EC cosmologies as our cosmic chronometers:

$$\begin{aligned}
\Lambda\text{CDM} : \tau_U &= \frac{9.7776}{h} \int_{10^{-3}}^1 \frac{da}{a} [\Omega_m a^{-3} + \Omega_\Lambda]^{-\frac{1}{2}} \text{Gyr}, \\
\text{EC} : \tau_U &= \frac{9.7776}{h} \int_{10^{-3}}^1 \frac{da}{a} [\Omega_m a^{-3} - \frac{1}{3} Q^2(a)]^{-\frac{1}{2}} \text{Gyr}, \\
\tau_U(\text{EC}) &\simeq \tau_U(\Lambda\text{CDM}) \\
\Rightarrow \frac{1}{h_1} [\Omega_{m,1} a^{-3} - \frac{1}{3} Q^2(a)]^{-\frac{1}{2}} &\simeq \frac{1}{h_2} [\Omega_{m,2} a^{-3} + 1 - \Omega_{m,2}]^{-\frac{1}{2}} \\
\Rightarrow Q(a) &= \sqrt{3} [(\frac{h_2}{h_1})^2 (\Omega_{m,2} - 1) + (\Omega_{m,1} - \Omega_{m,2}) (\frac{h_2}{h_1})^2 a^{-3}]^{\frac{1}{2}} \\
\Rightarrow Q(a) &= \sqrt{3} [-c_1 + c_2 a^{-3}]^{\frac{1}{2}} \simeq \sqrt{3c_2} a^{-\frac{3}{2}} [1 - \frac{c_1}{2c_2} a^3 + \dots].
\end{aligned}$$

We neglect very small terms with vorticity [21]. The resulting expression for angular momentum coincides with the evolution of the angular momentum of galaxies in the Zeldovich model [3]. Our final parametrization of torsion has the form (two redshifts are introduced to simulate a smooth rise of torsion):

$$\begin{aligned}
Q(a) &= \sqrt{3} (1 + \frac{a - a_0}{a_0 - a_1}) [1 - c + ca^{-3}]^{\frac{1}{2}}, \text{ for } a_1 \leq a \leq a_0, \\
a &= \frac{1}{1+z}, \quad a_0 = \frac{1}{1+z_0}, \quad a_1 = \frac{1}{1+z_1}, \\
Q(a) &= \sqrt{3} [1 - c + ca^{-3}]^{\frac{1}{2}}, \text{ for } a_0 \leq a \leq 1, \\
\Omega_Q &= -1 \iff Q(a=1) = \sqrt{3}, \quad Q(a \leq a_1) = 0.
\end{aligned}$$

In Table 1 we summarize parameters of models.

The equation for the growth function $D_+(a)$ within the EC cosmology can be easily derived [21]:

$$\Lambda\text{CDM} : \delta(a) = \frac{\sqrt{1+x^3}}{x^{3/2}} \int_{10^{-3}x_0}^x \frac{dx x^{3/2}}{(1+x^3)^{3/2}},$$

$$\begin{aligned}
x &= x_0 a, \quad x_0 = \left(\frac{\Omega_\Lambda}{\Omega_m}\right)^{1/3}, \\
EC : \frac{d^2 \delta}{da^2} &= (\dot{a})^{-2} \left[-(\ddot{a} + 2\frac{\dot{a}^2}{a}) \frac{d\delta}{da} + \frac{3}{2} \frac{\dot{a}^2}{a^2} \delta \right], \\
\frac{\dot{a}^2}{a^2} &= H_0^2 \left[\Omega_m a^{-3} - \frac{1}{3} Q^2(a) \right], \quad \frac{\ddot{a}}{a} = H_0^2 \left[-\frac{1}{2} \Omega_m a^{-3} + \frac{2}{3} Q^2(a) \right], \\
D_+(a) &\equiv \frac{\delta(a)}{\delta(1)}, \quad H_0 = 100h \text{ km s}^{-1} \text{ Mpc}^{-1}.
\end{aligned}$$

Figure 1 describes the quotient of the growth functions for EC and Λ CDM models.

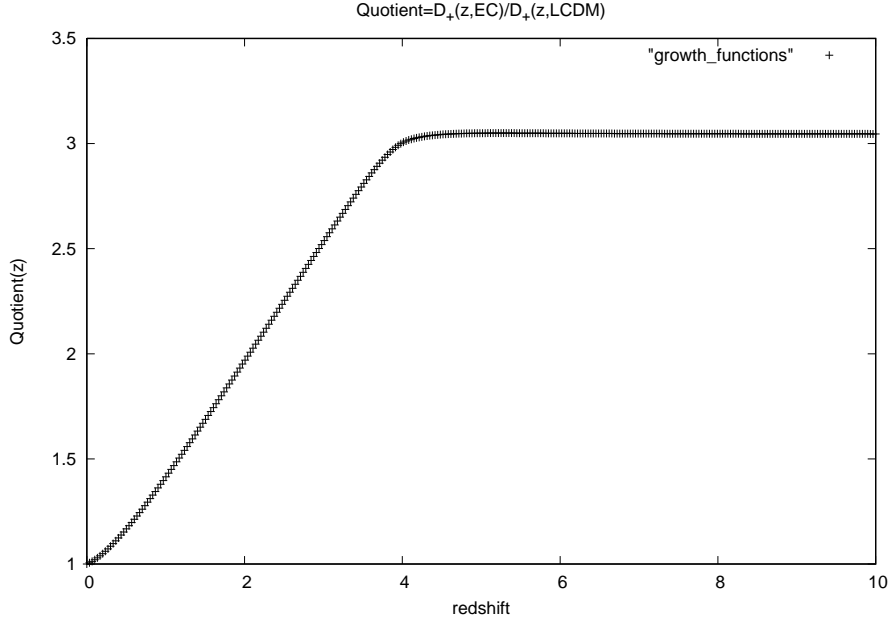


Fig. 1. Quotient of growth functions $D_+(z, EC)/D_+(z, \Lambda CDM)$

4. High-redshift Universe

With a rapid growth of our knowledge based on new measurements and more precise theoretical computations, cosmologists are faced with the first large discrepancy of the Λ CDM model: accurate measurements of the Hubble parameter in our "local" (very small redshift) Universe vs. fit of the Hubble parameter with CMB data (evolution from $z_{dec} \simeq 1100$ to $z = 0$), with galaxy clustering at various redshift, with gravitational lenses, etc.

This is a clear evidence that the Λ CDM model with cold dark matter, cosmological constant and isotropic and homogeneous FRW geometry does not describe the physical reality any more. We mentioned already the lack of power of the TT CMB spectrum at large scales. This topic deserves a separate investigation, however it is no more a surprise in light of the "Hubble tension".

We choose an observable that is well measured and redshift dependent: the galaxy halo number density. The evaluation requires our choice of primordial density spectrum, processed spectrum imprinted in transfer functions, fitting functions and growth functions. The Harrison-Zeldovich-Peebles primordial spectrum [1, 2, 3, 4] with a small tilt [25, 26, 27] is applied:

$$P(k, z) = CP_i(k)T^2(k)D_+^2(z), \quad C = \text{normalization constant},$$

$$P_i(k) = k^\alpha, \quad \alpha = 0.96, \quad T(k) = \text{transfer function}.$$

Since both Λ CDM and EC models assume the adiabatic CDM perturbations, we use the corresponding transfer function as a result of the integrated Boltzmann equations with CDM, baryons and photons (small corrections of light neutrinos are neglected)[4]:

$$T(k) = \frac{\ln(1 + 2.34q)}{2.34q} [1 + 3.89q + (16.1q)^2 + (5.46q)^3 + (6.71q)^4]^{-1/4},$$

$$q = \frac{k}{(\Gamma h Mpc^{-1})}, \quad \Gamma = h\Omega_m \exp[-\Omega_b(1 + \sqrt{2h}/\Omega_m)].$$

The fitting functions are defined by probability calculations of high-density regions [3] and we choose the Sheth-Tormen function because of its universal applicability with respect to halo mass and redshift [28]:

$$f_{ST}(\sigma) = A\sqrt{\frac{2r}{\pi}} \left[1 + \left(\frac{\sigma^2}{r\delta_c^2}\right)^p\right] \frac{\delta_c}{\sigma} \exp\left[-\frac{r\delta_c^2}{2\sigma^2}\right],$$

$$A = 0.3222, \quad \delta_c = 1.686, \quad r = 0.707, \quad p = 0.3,$$

$$\int_{-\infty}^{+\infty} f_{ST}(\sigma) d \ln \sigma^{-1} = 1.$$

The growth functions are evaluated in the preceding section and we are now equipped with all the necessary ingredients to evaluate galaxy halo number density as a function of halo mass and redshift [4]:

Table 2. Halo number density as a function of mass and redshift;
 upper number= $\frac{dn}{dM}(EC; Mpc^{-3}M_{\odot}^{-1})$, lower number= $\frac{dn}{dM}(EC) / \frac{dn}{dM}(\Lambda CDM)$.

$z \setminus M(M_{\odot})$	10^9	10^{10}	10^{11}	10^{12}
	$4.06 \cdot 10^{-9}$	$5.59 \cdot 10^{-11}$	$8.09 \cdot 10^{-13}$	$1.25 \cdot 10^{-14}$
4	4.26	6.38	13.18	55.61
	$4.78 \cdot 10^{-9}$	$6.60 \cdot 10^{-11}$	$9.57 \cdot 10^{-13}$	$1.47 \cdot 10^{-14}$
6	7.79	16.66	66.29	1048.36
	$5.45 \cdot 10^{-9}$	$7.53 \cdot 10^{-11}$	$1.09 \cdot 10^{-12}$	$1.65 \cdot 10^{-14}$
8	18.30	63.08	602.52	55574.74

$$\begin{aligned} \frac{dn(M, z)}{dM} &= f_{ST}(\sigma) \frac{\bar{\rho}_m(z=0)}{M} \frac{d \ln \sigma^{-1}}{dM}, \\ \bar{\rho}_m(z) &= \Omega_m (1+z)^3 \rho_{crit}(z=0), \quad M = \frac{4\pi \bar{\rho}_m(z=0)}{3} R^3, \\ \sigma^2(R, z) &= \frac{1}{2\pi^2} \int_0^{+\infty} dk k^2 P(k, z) W^2(kR), \quad \rho_{crit}(z=0) = \frac{3H_0^2}{8\pi G_N}, \\ \sigma &= \text{variance}, \quad W(x) = \text{window function} = \frac{3}{x^3} (\sin x - x \cos x). \end{aligned}$$

It is easy to verify that:

$$\begin{aligned} \frac{d \ln \sigma^{-1}}{dM} &= -\frac{3}{2\pi^2 M \sigma^2 R^4} \int_0^{+\infty} dk k^{-2} P(k, z) \\ &\times (\sin kR - kR \cos kR) \left[\sin kR \left(1 - \frac{3}{(kR)^2} \right) + 3 \frac{\cos kR}{kR} \right]. \end{aligned}$$

We present results for Λ CDM and EC models normalizing the spectrum by the standard method with a variance $\sigma_8 = \sigma(R_8 = h^{-1}8Mpc, z=0) = 0.823$.

The evaluations of the halo number density for halo masses from 10^9 to $10^{12}M_{\odot}$ and for redshifts from $z=4$ to $z=8$ depicted in Table 2 and Figure 2 clearly show large enhancements in EC cosmology with respect to Λ CDM model.

This phenomenon is observed few years ago [29] and does not vanish with new observations [30]. A disparity between Λ CDM and EC models weighing few orders of magnitude should not be considered as a surprise since the

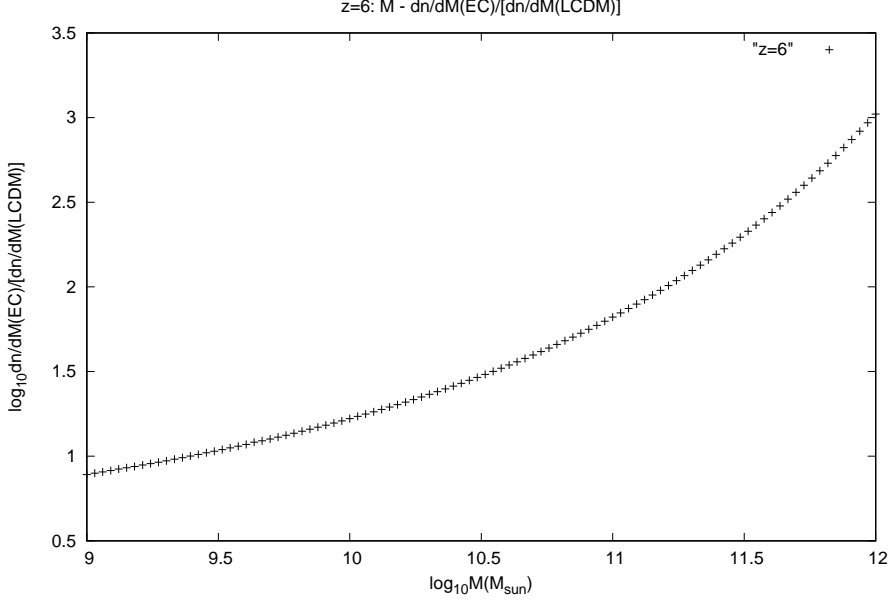


Fig. 2. redshift=6: $\log_{10}M(M_{\odot})$ vs. $\log_{10}[\frac{dn}{dM}(EC)/\frac{dn}{dM}(\Lambda\text{CDM})]$

high-density regions follow probability rules in the form of the exponential fitting functions. One can conclude that current measurements, albeit with limited statistics for higher redshifts, support the EC model.

The first measurement of the cosmic 21-cm absorption signal from the neutral hydrogen transition of EDGES [31] came as a surprise. Namely, the absorption signal at redshift $z = 17.2$ appears to be much stronger than it is anticipated from the standard brightness temperature contrast of the spin temperature against the CMB [32, 33] for ΛCDM model:

$$\delta T_b \approx 20\text{mK} \left(1 - \frac{T_{cmb}(z)}{T_s(z)}\right) \frac{x_{HI}(z)(1+\delta)}{1 + \frac{dv_r}{dr}/H(z)} \sqrt{\frac{1+z}{10}} \frac{0.15}{\Omega_m h^2} \frac{\Omega_b h^2}{0.023},$$

$$\delta T_b(z \approx 17; \text{EDGES}) \approx -500\text{mK}, \quad \delta T_b(z \approx 17; \Lambda\text{CDM}) \approx -220\text{mK}.$$

One can reconcile the theory and measurements with cooling the intergalactic medium (IGM) ($T_k \simeq T_s$) or adding to T_{cmb} large radio background temperature T_{rad} at the EDGES signal redshift. Applying one of the standard recombination codes to the EC model, we estimate T_k at $z \simeq 17$ [34] to be only 10% cooler than T_k of ΛCDM . This is understandable from the corresponding evolution equation for T_k (the second term with a Compton heat-

ing has larger ionization fraction \bar{x}_i in the numerator but also larger square root of the mass density parameter $H(z) \propto \sqrt{\Omega_m}$ in the denominator)[34]:

$$\frac{dT_k}{dz} = \frac{2T_k}{1+z} + \frac{8\sigma_T u_{cmb}}{3m_e c(1+z)H(z)} \frac{\bar{x}_i}{1+f_{He}+\bar{x}_i} (T_k - T_{cmb}).$$

Therefore, the EC model has even smaller 21-cm absorption signal $\delta T_b(z \approx 17; EC) \approx -100 mK$.

Feng and Holder [35] proposed recently the inclusion of the additional radio background that can resolve the problem with the EDGES signal, i.e. $T_{radio} \simeq few T_{cmb}$. We comment on three thorough analyses of the first galaxies [36, 37, 38] and their impact on the 21-cm signal. The first paper [36] investigates the first black holes in mini-halos, their accretion rates and implications on radio, infrared, X-ray and CMB backgrounds, as well their impact on possible heating of the intergalactic medium (T_k). The second paper [37] deals with the early atomic-cooling galaxies, modeling radiative processes and taking care of all cosmological constraints. The third paper [38] describes the first nonlinear structures as molecularly cooled mini-halo galaxies. The extensive numerical analyses in these papers are performed within Λ CDM cosmology.

Although all three analyses are based on large number of uncertain parameters, functions and procedures, one can notice one common conclusion: it is possible to reproduce the EDGES absorption signal but with very unusual X-ray source efficiencies that should be $\mathcal{O}(10^3)$ larger than expected. A key ingredient in analyses is the luminosity function which is proportional to the number density of halos. If we compare number densities for mini-halos in EC and Λ CDM at redshift range $z \in [15, 25]$ one can see in Table 3 the amplification of $\mathcal{O}(10^2) - \mathcal{O}(10^4)$ in favour of the EC model, precisely what we need to explain the absorption signal.

At the end of this section we point to new measurements and analysis [39] of ionizing photon mean free path at redshift $z = 6$ resulting in "increased demands on ionizing sources" in Λ CDM model. The EC model (see Table 2) has larger number of ionizing sources.

5. Conclusions

With great progress in precision and high-redshift measurements in astrophysics confronted with more powerful simulations and calculations, we are faced with severe problems of the concordance Λ CDM cosmology. The EC cosmology with CDM and light neutrinos represents a possible natural path to resolve problems of high-redshift Universe. The effects of torsion through spin and angular momentum densities are backbones of the new

Table 3. Mini-halo number density as a function of mass and redshift;
upper number= $\frac{dn}{dM}(EC; Mpc^{-3}M_{\odot}^{-1})$, lower number= $\frac{dn}{dM}(EC) / \frac{dn}{dM}(\Lambda CDM)$.

$z \setminus M(M_{\odot})$	10^5	10^6	10^7	10^8
15	0.359	$3.45 \cdot 10^{-3}$	$4.32 \cdot 10^{-5}$	$4.94 \cdot 10^{-7}$
	9.35	17.15	60.02	214.68
20	0.413	$3.98 \cdot 10^{-3}$	$4.98 \cdot 10^{-5}$	$5.69 \cdot 10^{-7}$
	39.65	114.41	777.94	7662.22
25	0.46	$4.45 \cdot 10^{-3}$	$5.57 \cdot 10^{-5}$	$6.34 \cdot 10^{-7}$
	256.20	1315.19	20792.48	741775.22

theoretical machinery. The violation of isotropy is already observed in the Planck TT CMB spectrum [40]. There is a hint for a parity violation in polarization data of Planck [41, 42] with a preference to right-handedness [22]. It could stimulate the theorists to undertake extensive numerical simulations with expanding and rotating Universe to reveal the redshift dependence of torsion from the first principles of the Einstein-Cartan cosmology.

REFERENCES

- [1] P. J. E. Peebles, *The Large-Scale Structure of the Universe*, Princeton University Press, Princeton 1980.
- [2] E. W. Kolb and M. S. Turner, *The Early Universe*, Addison-Wesley, Redwood City 1990.
- [3] T. Padmanabhan, *Structure formation in the universe*, Cambridge University Press, Cambridge 1995.
- [4] J. A. Peacock, *Cosmological Physics*, Cambridge University Press, Cambridge 1999.
- [5] D. Palle, *Nuovo Cim. A* **109**, 1535 (1996).
- [6] D. Palle, *Nuovo Cim. B* **115**, 445 (2000).
- [7] K. Griest, M. Kamionkowski, *Phys. Rev. Lett.* **64**, 615 (1990).
- [8] M. Fukugita, T. Yanagida, *Phys. Lett. B* **174**, 45 (1986).
- [9] A. D. Sakharov, *JETP Lett.* **5**, 24 (1967).
- [10] D. Palle, *Acta Phys. Pol. B* **43**, 1723 (2012).
- [11] D. Palle, "On the quantum loop suppressed electroweak processes", arXiv:1210.4404.
- [12] D. Palle, *Hadronic J.* **24**, 87 (2001).
- [13] D. Palle, *Acta Phys. Pol. B* **43**, 2055 (2012).

- [14] P. Cea, "Comment on the evidence of the Higgs boson at LHC", arXiv:1209.3106.
- [15] D. Palle, "On the possible new 750 GeV heavy boson resonance at the LHC", arXiv:1601.00618.
- [16] A. Heister, "Observation of an excess at 30 GeV in the opposite sign di-muon spectra of $Z \rightarrow b\bar{b} + X$ events recorded by the ALEPH experiment at LEP", arXiv:1610.06536.
- [17] T. W. B. Kibble, *J. Math. Phys.* **2**, 212 (1961); D. W. Sciama, *J. Math. Phys.* **2**, 472 (1961).
- [18] A. Trautman, *Nature* **242**, 7 (1973).
- [19] D. Palle, *Nuovo Cim. B* **111**, 671 (1996).
- [20] D. Palle, *Nuovo Cim. B* **114**, 853 (1999).
- [21] D. Palle, *Eur. Phys. J. C* **69**, 581 (2010).
- [22] D. Palle, *Entropy* **14**, 958 (2012).
- [23] Yu. N. Obukhov, V. A. Korotky, *Class. Quant. Grav.* **4**, 1633 (1987).
- [24] R. Penrose, *Proc. Roy. Soc. Lond. A* **284**, 159 (1965).
- [25] WMAP Collab., *ApJ Suppl.* **170**, 377 (2007).
- [26] D. Palle, *Nuovo Cim. B* **122**, 67 (2007).
- [27] Planck Collab., *A & A* **594**, A13 (2016).
- [28] R. K. Sheth, G. Tormen, *MNRAS* **308**, 119 (1999).
- [29] C. L. Steinhardt et al., *ApJ* **824**, 21 (2016).
- [30] D. R. Riechers et al., *ApJ* **895**, 81 (2020); M. L. Stevans et al., "The NEW-FIRM HETDEX Survey", arXiv:2103.14690, to appear in *ApJ*.
- [31] J. D. Bowman et al., *Nature* **555**, 67 (2018).
- [32] S. R. Furlanetto, S. P. Oh, F. H. Briggs, *Phys. Rep.* **433**, 181 (2006).
- [33] J. R. Pritchard, A. Loeb, *Rep. Prog. Phys.* **75**, 086901 (2012).
- [34] S. Seager, D. D. Sasselov, D. Scott, *ApJ Suppl.* **128**, 507 (2000).
- [35] C. Feng, G. Holder, *ApJ* **858**, L17 (2018).
- [36] A. Ewall-Wice et al., *ApJ* **868**, 63 (2018).
- [37] J. Mirocha, S. R. Furlanetto, *MNRAS* **483**, 1980 (2019).
- [38] Y. Qin et al., *MNRAS* **495**, 123 (2020).
- [39] F. B. Davies et al., "The Predicament of Absorption-Dominated Reionization: Increased Demands on Ionizing Sources", arXiv:2105.10518.
- [40] Planck Collab., *A & A* **594**, A16 (2016).
- [41] Y. Minami, E. Komatsu, *Phys. Rev. Lett.* **125**, 221301 (2020).
- [42] V. A. Korotky, Yu. N. Obukhov, *JETP* **72**, 11 (1991); V. A. Korotky, Yu. N. Obukhov, *JETP* **81**, 1031 (1995).